


Research Article

Structural Weight and Stiffness Optimization of a Midibus Using the Reinforcement and Response Surface Optimization (RSO) Method in Static Condition

Hailemichael Solomon Addisu ^{1,2} and Ermias Gebrekidan Koricho³

¹*School of Mechanical and Industrial Engineering, Addis Ababa Institute of Technology, Addis Ababa University, Addis Ababa, Ethiopia*

²*School of Mechanical and Industrial Engineering, Institute of Technology, Dire Dawa University, Dire Dawa, Ethiopia*

³*Department of Mechanical Engineering, Georgia Southern University, Georgia, USA*

Correspondence should be addressed to Hailemichael Solomon Addisu; hailemichael.solomon@aait.edu.et

Received 27 August 2021; Revised 25 December 2021; Accepted 31 December 2021; Published 1 February 2022

Academic Editor: Angelos Markopoulos

Copyright © 2022 Hailemichael Solomon Addisu and Ermias Gebrekidan Koricho. This is an open access article distributed under the Creative Commons Attribution License, which permits unrestricted use, distribution, and reproduction in any medium, provided the original work is properly cited.

Midibuses are medium-sized buses widely used for transportation purposes in Asia and Africa. However, most midibuses are locally built and indirectly regulated through inspecting the end product (finished bus) during licensing for the public transport business in Ethiopia. Due to lack of engineering analysis and testing, low stiffness and overweight of midibus were compromised. This research was aimed at analyzing and optimizing the midibus structure using the reinforcement and response surface optimization (RSO) method for pure bending and torsion loading cases. Results show that the maximum deformation occurred at the roof section of the original structure during both loading cases. Furthermore, the reinforcement design was found by replacing the cross section and layouts of structural members and adding reinforcements for the most suitable location of the original structure. Response surface optimization with the multiobjective genetic algorithm (MOGA) method in ANSYS DesignXplorer was performed on the reinforced structure to maximize the bending and torsional stiffness with reduced weight. The bending stiffness of the reinforced and optimized structure increased by 41.65% (1911.4 N/m) and 10.02% (651.7 N/m), respectively. In addition, the torsional rigidity or stiffness of the bus structure was improved by 12.56% (173.31 Nm/deg) via reinforcement design. Moreover, the torsional stiffness of the optimized (RSO) model was increased by 3.29% (51.07 Nm/deg). Reinforcement design was effectively reduced by 5.23% of the structure's weight. Moreover, the RSO method has also decreased the weight of the reinforced structure by 2.64%.

1. Introduction

Structural optimization mainly focuses on determining the optimal size and shape of the structure by the iterative approach [1]. Moreover, the response surface optimization combined with the MOGA (multiobjective genetic algorithm) optimization algorithm can develop the multiobjective optimization of the design parameters to obtain the optimal solution for static stiffness and weight of the structure. According to Zhang et al. [2], the MOGA optimization algorithm in the response surface method (RSM) is targeted to reduce the mass,

maximum deformation, and natural frequencies of the electric vehicle frame using ANSYS Workbench.

Crocco et al., Reyes-ruiz et al., Rooppakhun and Wichairahad, and Wang et al. [3–6] conducted a static structural analysis of bus structure using the FE (finite element) method under bending and torsion loading conditions. Moreover, Lan et al. [7] discussed the experimental and numerical analyses of bus structure strength and structural design optimization. According to Yang et al. [8], the bus's weight is reduced by changing the frame of a bus structure for a lightweight design. Furthermore, Wu et al. [9] investigated the

frame distribution as a truss on the sidewall of the bus to strengthen the bus structure with weight reduction during bending and torsion conditions. Pravalonis et al. [10] discovered that frame strength and stiffness are indicators for the behavior of bus structures. Ismail et al. [11] focused on the response surface optimization (RSO) method to obtain a better optimal design in the static structural analysis of a three-dimensional bike crank arm. According to Gauchia and Diaz and Zhong et al. [12, 13] showed that a genetic algorithm (GA) is a well-matched optimization approach to reduce the weight and increase the torsional stiffness in very complex problems. Moreover, Kim [14] also focused on the weight optimization of the bus structure by changing the thickness of the frames, although filling the constrained torsional and bending values simultaneously. Previous research shows that the strength parameters of the bus superstructure and structural optimization for lightweight design are crucial during experimental and numerical studies.

Feng et al. [15] carried out the thickness optimization of the bridge by setting up the multiobjective genetic algorithm (GA) procedures in ANSYS. Kang et al. [16] considered the optimal design of an impeller shroud for a centrifugal compressor using the response surface method (RSM) with the multiobjective genetic algorithm (MOGA). Muhammad et al. [17] proposed the topology (weight) optimization of the connecting rod with a target weight reduction of 20%-60% to minimize weight and cost using ANSYS Workbench. Moreover, a response surface optimization (RSO) was done by varying the rod pin end diameter and bearing diameter. Moreover, Mi et al. [18] developed the function of multiobjective optimization to reduce the weight of an A-type frame and improve the reliability of fuzzy fatigue in an electric mining dump truck. Furthermore, Hadadian et al. [19] studied the response surface functions for the magnetic field intensity across the activation length of a magnetorheological valve orifice using the combination of the FE model and response surface techniques. According to Boada et al. [20], the optimization of weight and torsional stiffness parameters of the bus structure through changing the thickness of beam was investigated using a combination of genetic algorithms (GA) in MATLAB and FE methods (ANSYS). Moreover, Choudhary et al. [21] focused on improving the ultimate strength of a circular cylindrical shell by the FE approach with MATLAB during several loading conditions.

Zhang et al. [22] studied the reduction of stress and stiffness of a novel integral squeeze film bearing damper (ISFBD) via a combination of the finite element and multiobjective optimization techniques by decreasing the transmitted force and usage of damping effect. Zheng et al. [23] studied brake drums' static and modal analysis using the finite element method with response surface optimization in ANSYS. Moreover, the multiobjective optimization of the drum weight and natural frequencies is conducted by changing the dimension of the brake drum. Ren et al. [24] demonstrated the response surface-based FE model in static structural analysis of the box-girder bridge via experimental and numerical approaches [24]. According to Wu et al. [25], the structural stiffness of the gravure hexagonal cell microstructure within a lightweight design was evaluated using

FE analysis (ANSYS Parametric Design Language (APDL)) based on the response surface optimization approach. Moreover, the optimization results via a multiobjective genetic algorithm (MOGA) indicated that the total volume and maximum deformation were reduced by 46.3% and 44.4%, respectively.

This research investigates the medium capacity bus (midibus) structure established by the local bus manufacturer in Ethiopia. In Ethiopia, most local bus manufacturers experience the design of the structure's construction through try and error methods, and this approach results in low structural strength and overweight of the bus. In this research, first, the existing bus structure is carefully examined through the manufacturer constraint and the static simulation using the FE method to select the components that might be modified. When this selected element leads to a high structural deformation with overweight, the structural components' substitution and modification (reinforcement) were considered. After reinforcement, the response surface optimization with the multiobjective genetic algorithm (MOGA) method was developed to reduce the weight and maximize the stiffness of the reinforced structure using a variation of shell thickness according to manufacturable value. Finally, the comparison of the original, reinforced, and optimized model was considered according to the structural weight and stiffness.

2. Methodology

2.1. Static Strength Analysis via the Finite Element (FE) Method. Most of the midibus bodies in Ethiopia are built on used and new truck chassis (Isuzu N-Series such as NPR (71H, 71K, and 66L), NQR, and FSR) using locally available materials. Mainly, the bodybuilders used Isuzu trucks to build a midibus using diverse methods. First, the midibus structure is constructed into six central (front, right-side, left-side, rear, floor, and roof) components and then joined with the chassis together. Next, the other approach is joining every part of the structure step by step from the chassis. In this research, the geometry of the midibus structure was developed by directly measuring and observing the bus construction from the available local manufacturers (bodybuilders) in Addis Ababa, Ethiopia. Moreover, the geometry of the locally midibus structure and NPR-71K model of the chassis is described as shown in Figure 1. However, this study does not analyze and evaluate the strength of the chassis body and its components.

The local manufacturer and legislator body stated that the mass of the unladen kerb (M_k) and gross vehicle weight (GVW) of the midibuses had 28 + 1 passenger capacity measured at 4400–4700 kg and 7200–7400 kg, respectively. Table 1 describes the overall specification of the selected midibus model. The structure frames are constructed and manufactured using the available materials, shapes, and cross sections. Moreover, as depicted in Table 1, the dimension (height (H), width (B), and thickness (T)) of cross sections according to the cross-sectional type is mentioned.

Moreover, the midibus structure cross sections (rectangular hollow section (RHS), square hollow section (SHS),

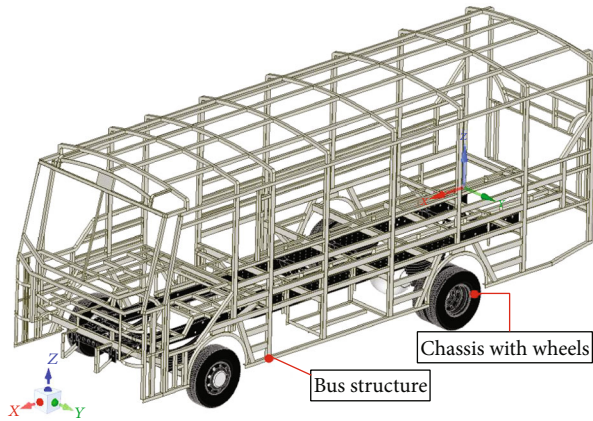


FIGURE 1: 3D geometry of the bus existing structure and chassis with wheels.

L-shape (angle steel), and U-shaped) have been clearly stated in Figure 2.

In this research, the static structural analysis of the midibus includes the bending and torsional strength via FE methods (ANSYS Software). Accordingly, the two load conditions are full pure bending and torsion. The bus structure's CAD model is developed in the Initial Graphics Exchange Specification (IGES) format as a surface and imported to ANSYS Software. The FE model of bus sections is constructed as a shell (shell_180) with mixed mesh (quadrilateral and triangular element), as shown in Figure 3. However, the body structures' maximum and minimum element sizes are 10 mm and 2.5 mm due to the small and large frame size. The FE model of the bus structure contains 553,040 elements and 572,578 nodes with 355 parts.

The connection of parts (regions) describes the movement of contacting bodies relative to one another [26]. Selecting the appropriate contact connection type depends on the problem type that wants to resolve it [27]. The bonded contact gives a glued contact region and efficiently applies to all connection regions for welded, bolted, and riveted parts in assemblies [27–32]. The structural parts of the midibus were interconnected (joining) by the shield metal arc welding method. This research defines the contact connections between structural components as a “bonded contact.” The material properties of structural steel are mentioned, as shown in Table 2. The material input data of the FE simulation needs the effective stress versus the effective plastic strain curve.

2.1.1. Static Loading and Boundary Conditions. First, the average values of the masses floor and roof luggage and chairs are taken per the local manufacturer standard (see Table 3). Then, the lumped masses of the side and roof luggage, driver, passengers, and seats are loaded on the structural parts. This study takes the driver and passenger mass of 75 kg as stated by local manufacturer and legislator standards.

In the pure bending case, the lumped masses of the floor and roof luggage, driver, passengers, and seats are distributed on the structural parts with gravitational force [3, 4].

According to the original midibus structure model, the realistic boundary conditions are applied between the chassis (chassis axles and frames) and structural frames, as shown in Figure 4. This case's fixed constraints are significantly located at the rear axle, front C-channel, and L-angle steels with a hole. The bending stiffness of the structure is the ratio of applied load and vertical deformation on a pure bending case [4, 33].

This case's fixed constraints are significantly located at the rear axle and front C-channel (support C), the engine side support (support H), and L-angle steels with a hole (support G) (see Figure 5).

The equation of bending stiffness (K_b) can be calculated by

$$K_b = \frac{W_b}{\delta y}, \quad (1)$$

where W_b is the applied load in the pure bending (N) and δy is the linear deformation (mm).

During the torsional loading case, the distributed masses are the same as those during the pure bending case, and torsional loads act on the structural parts with gravitational force [3, 6, 34]. However, the torsional loads are obtained from the total reaction forces (5,309.2 N) of the bending case's four-axle points. The torsional loads are applied for each frontal C-channel connected with nodes (nodal forces G and H) as a value of 1,327.3 N, as shown in Figure 6. The boundary conditions are applied at the rear axle (fixed support E), engine frames connected to the chassis (fixed support J), and the L-shaped parts bolted with the chassis (fixed support I). The moment (couple) acting on the hinges is defined as the applied force multiplied by the perpendicular distance from the center of the lateral axis of the structure.

The moment acts in the two sides of the front (axle) steering system as a couple. Therefore, the total moment (torque) T_m becomes

$$T_m = \text{Applied Force} \times L. \quad (2)$$

The torsional stiffness or rigidity of the structure (K_t) is calculated by

$$K_t = \frac{T_m}{\theta}, \quad (3)$$

$$\theta = \tan^{-1} \left(\frac{\delta y}{L/2} \right),$$

where δ is the angle of rotation (degree), L is the distance between the two sides of frontal wheel supports (mm) (see Figure 6(b)), and δy is the total deformation (mm).

2.2. Reinforced Design and Optimization Method. Optimization is the development of objective function with constraints to maximize or minimize the desired value [35]. The numerical simulation requires many iterations and design parameters during the numerical optimization process [36]. However, the reinforcement of the vehicle body

TABLE 1: General specification of the midibus (NPR 71K chassis) with the size of cross sections.

Overall dimension (mm)		Unladen kerb mass (M_k) (kg)		Gross vehicle weight (GVW) (kg)
Length (l)	Width (w)	Height (h)		
7250	2880	2580	4500	7350
Sizes of cross sections (in mm)				
RHS tubes ($H \times B \times T$)	SHS tubes ($H \times B \times T$)	L-angle ($H \times B \times T$)	C-shaped ($H \times B \times T$)	U-shaped ($H \times B \times T \times h$)
$60 \times 40 \times 1.5$	$40 \times 40 \times 1.5$	$40 \times 40 \times 1.5$	$70 \times 40 \times 5$	$70 \times 40 \times 1.5 \times 16.5$
$60 \times 50 \times 3$	$40 \times 40 \times 3$	—	—	—

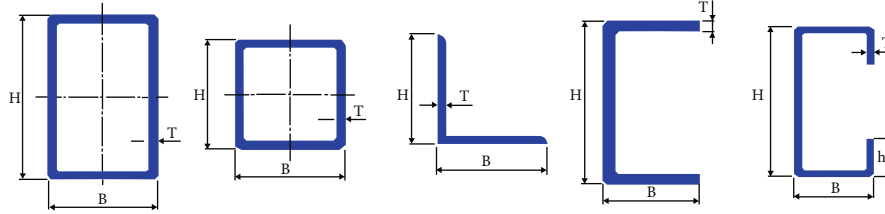


FIGURE 2: Geometrical configurations of cross sections.

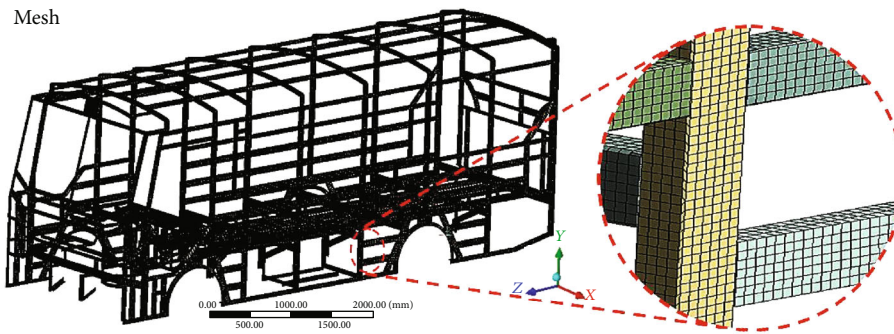


FIGURE 3: FE discretization of the structure.

TABLE 2: Mechanical property of conventional structural (CS) steel.

Material type	Density (kg/mm ³)	Yield strength (MPa)	Tensile strength (MPa)	Elongation (%)	Young's modulus (GPa)	Poisson's ratio, ν
CS steel	7850	260	360	30	210	0.3

TABLE 3: Sum of masses applied on the bus structure.

Categories	Qty.	Total mass (kg)
Passengers with the driver (each 75 kg)	29 + 1	2250
Seat (each 8.5 kg)	29 + 1	255
Floor (side+rear) luggage	—	200
Roof luggage	—	350

is one of the optimization techniques to strengthen the vehicle's body [37]. Thus, this research is aimed at providing the reinforced and optimized design using reinforcement and numerical optimization (response surface optimization with MOGA) methods.

2.2.1. Reinforced Design via the Reinforcement Approach. As shown in Figure 7, most local bus bodybuilders used the wall support (U-channel) to support the wall and cover the skin of the bus from vibration. However, the weight of the bus structure increases due to the high numbers of wall support. Moreover, these components are not designed to connect (support) windows and waist rail. The other design defect from the manufacturer's side is that at the end of the chassis, the rear portion of the bus extends around 500–700 mm to obtain more seats in the rear section. This design consideration eliminates the connection between the chassis body and floor section.

The existing bus structure needs strength analysis and improved design. In this research, the design modification (reinforcement) is conducted by adding and replacing the structural parts. The first approach concerns the layout of

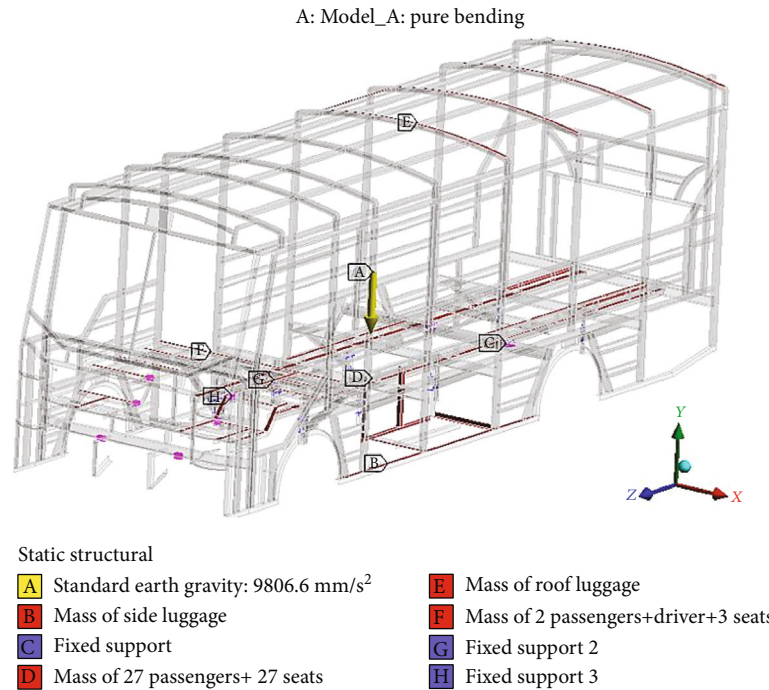


FIGURE 4: Pure bending load with boundary condition.

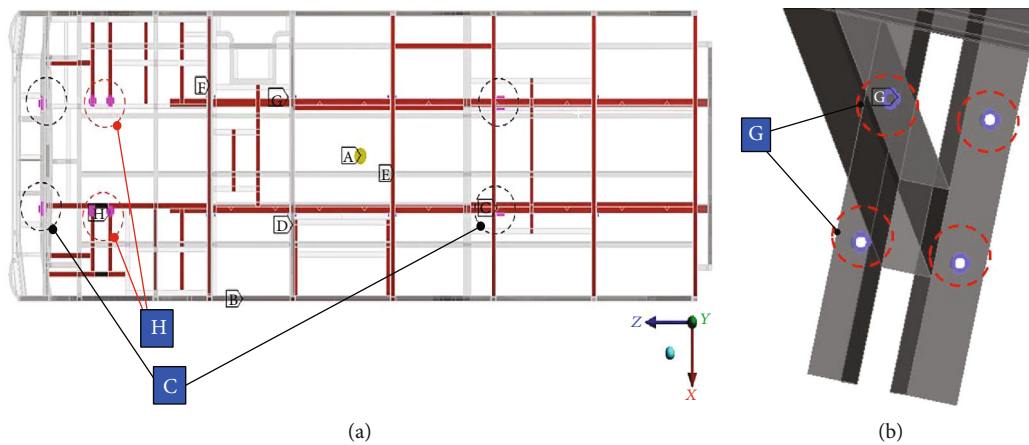


FIGURE 5: Fixed constraints through a pure bending case: (a) support C and H and (b) support G.

the structure and the shape of the cross section in the structural parts, as shown in Figure 8.

Next, the addition of supports was considered to assemble the structure section. Hence, the supporting member is attached at the corner of the floor and sidewall section on the rear portions to reduce the structural deformation. Moreover, the connecting elements on both side sections are constructed by using inclined square cross sections (SHS). The original structure contains maximum deformation at the end of the roof and floor section from the results of static strength analysis. However, the above design defects improve through additional support members (SM) using square hollow sections (SHS) and L-shaped cross sections, as shown in Figure 8.

Moreover, the roof arc members are replaced by rectangular hollow sections (RHS). Table 4 describes cross-

sectional types and masses of the components of enhanced configurations. In sum, this model decreases its weight by 29.98 kg compared to the original model.

2.2.2. Response Surface Optimization (RSO) in the Static Loading Case. Parametric optimization can be used to help designers determine the optimal sizes and shape of a structure using independent design variables (thickness, length, and coordinates) [26, 38].

Response surface optimization method is used for parametric optimization by considering the effect of design variables on the objective function [39]. Response surface optimization (RSO) procedures were conducted to increase the bending stiffness and weight reduction of the structure in pure bending, as shown in Figure 9. First, the reinforced design of the structure is parameterized by the thickness,

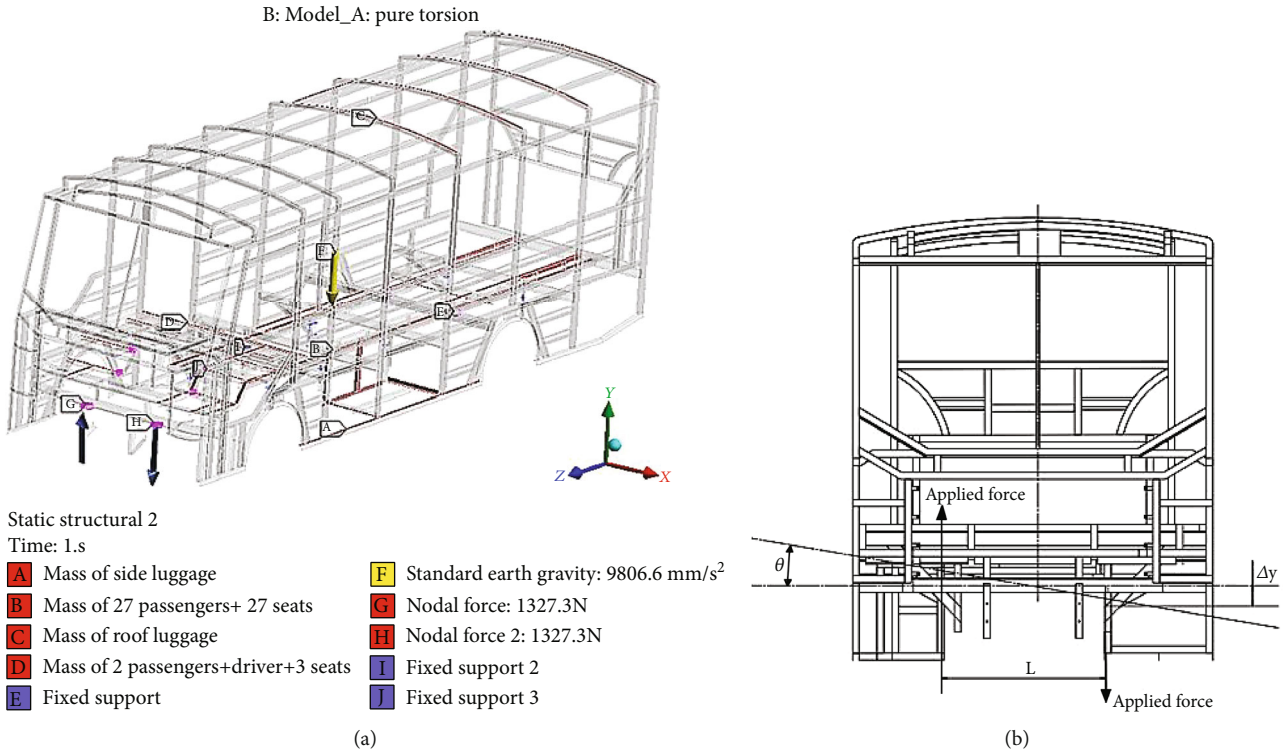


FIGURE 6: Loading and boundary condition: (a) pure torsional loading and boundary condition and (b) applied torsional force at a front view.

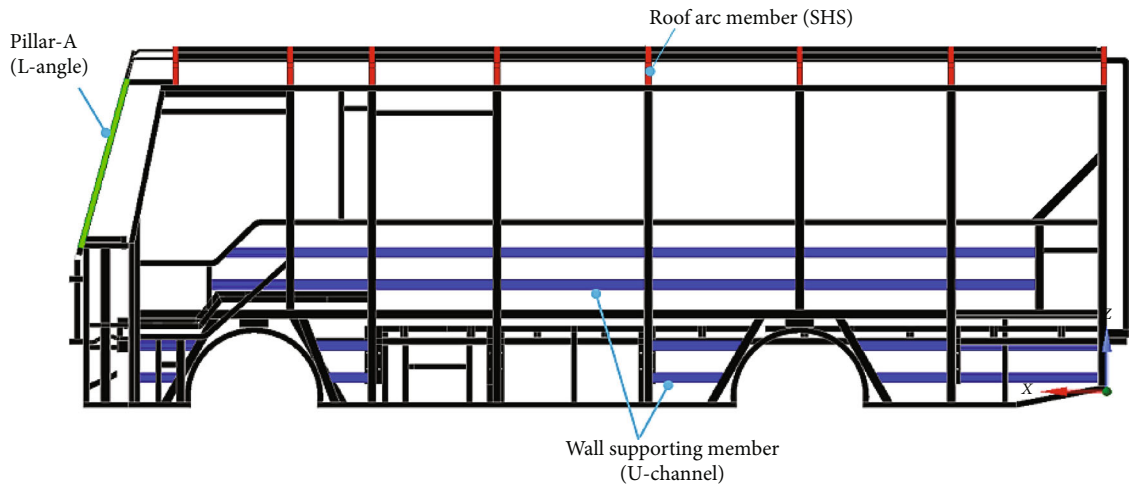


FIGURE 7: Selected configurations of the original design in a side view.

mass, and total deformation of the selected nine parts of the roof and floor section. Next, the ANSYS DesignXplorer develops the one hundred thirteen (113) experimental runs with five manufacturable thickness values using a faced-centered central composite design. Design of experiments is a method used to make the simulated response data suitable for the experimental data or mathematical equations in design optimization [26, 40]. An appropriate choice of components of structure bound by optimization is vital to declare rational optimization analysis [14].

During the static strength FE analysis of the reinforced structure, the maximum total deformation occurs at the roof section's four parts (P27, P28, P32, and P33). Furthermore,

the minimum deformation occurred at the floor section (P1–P5) in all loading cases, as shown in Figure 10. These parts are only selected to optimize the reinforced structural design because multiple variables with many levels require many simulation runs in numerical optimization. Figure 11 depicts the geometrical illustration of nine selected parts of the reinforced structure.

Moreover, Table 5 describes the cross-sectional types with the thickness of the selected parts with specified ranges of manufacturable values.

In this research, nine input variables (P1–P5, P27, P28, P32, and P33) at five manufacturable levels (1, 1.5, 2, 2.5, and 3 mm) need 113 design points (experimental runs), as

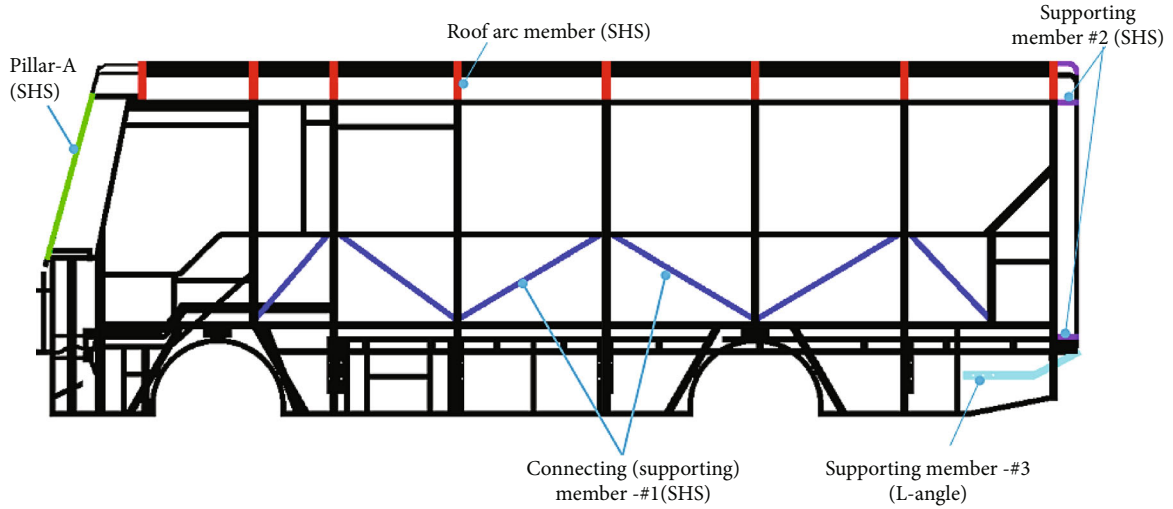


FIGURE 8: Enhanced configurations of the reinforced design in a side view.

TABLE 4: Components with its mass of enhanced configuration.

Description	Components					
	Front inclined pillar	Roof arc member	SM-#1	SM-#2	SM-#3	SM-#4
Cross section	SHS	RHS	SHS	SHS	L-angle	RHS
Qty.	2	8	11	5	2	12
Mass (kg)	4.53	44.74	19.7	2.58	7.86	6.12

SM-#1: supporting member-#1.

shown in Figure 12. A faced-centered central composite design (CCD) is a common experiment type due to its efficiency when providing much information within a minimum number of experiments [26]. Moreover, the one hundred thirteen (113) DOE points take more than five days (120 h) of computing time by using the Intel® Core™ i7-7700HQ CPU @ 2.80 GHz processor with 16 GB RAM.

After the experimental runs, the responses (maximum deformation and mass results) are obtained through the FE simulation for design scenarios. Each scenario dataset was used to correctly fit the response surface models.

As depicted in Figure 13, these response surface models provide various responses about design variables (thickness of the parts). Moreover, in the case of two variables (P27 and P28), their thickness gives the maximum deformation response of 4.15–4.2 mm, as shown in Figure 13(a). However, Figure 13(b) displays that the response deformation of 4.0–5.75 mm can be obtained from the two thickness variables (P32 and P33).

The response surface (RS) model can be validated by checking the fitting performance on design points [24]. The goodness of fit (correlation matrix) is calculated for the design of experiment points to check the accuracy of the response surface. As shown in Figure 14, most points fall on the lines, which means that the response surface can predict most of the design points within its ranges. Thus, it is possible to conclude that the predictable response surface is a pretty good fit for the observed design points. The ANSYS statistical metrics use the coef-

ficient of determination (R^2), root mean square error (RMSE), relative maximum absolute error (RMAE), and relative average absolute error (RAAE) in the calculations of the goodness of fit.

Coefficient of determination (R^2):

$$R^2 = 1 - \frac{\sum_{j=1}^N (r_j - \tilde{r}_j)^2}{\sum_{j=1}^N (r_j - \bar{r})^2}, \quad (4)$$

where r_j is the value of the output parameter in the j^{th} sampling point, \tilde{r}_j is the value of the regression model at the j^{th} sampling point, \bar{r} is the arithmetic mean of the values of r_j , and N is the number of sampling points.

Root mean square error (RMSE):

$$\text{RMSE} = \sqrt{\frac{1}{N} \sum_{j=1}^N (r_j - \tilde{r}_j)^2}. \quad (5)$$

Relative maximum absolute error (RMAE):

$$\text{RMAE} = \frac{1}{\sigma_r} \max_{j=1:N} |r_j - \tilde{r}_j|, \quad (6)$$

where σ_r is the standard deviation of r_j values.

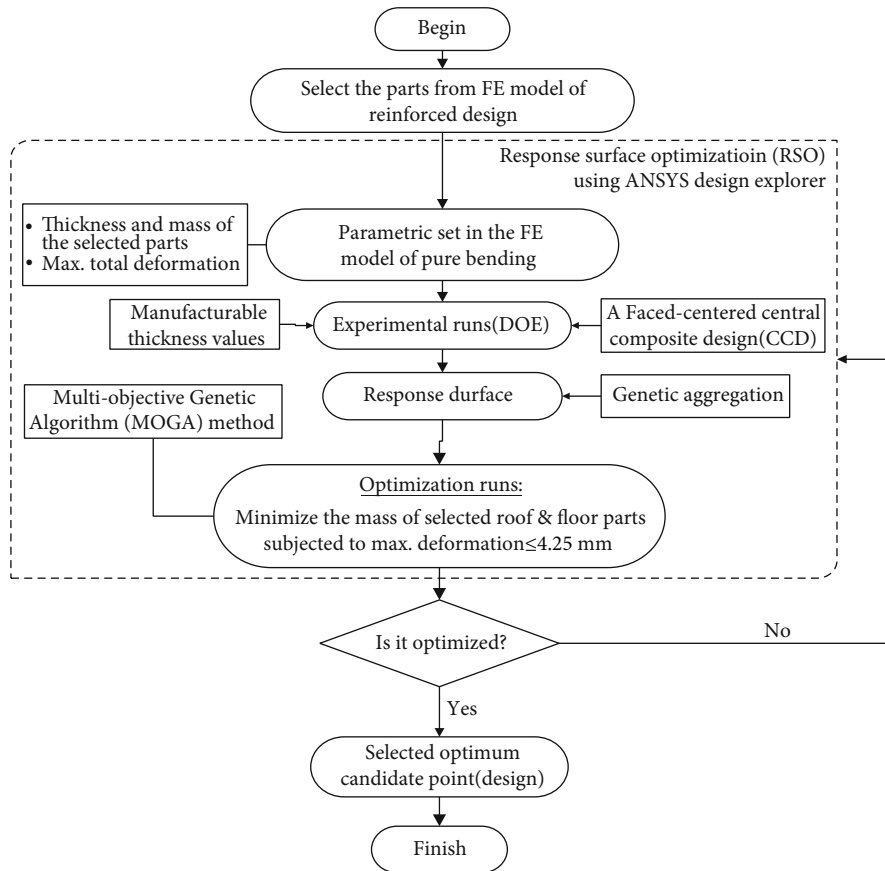


FIGURE 9: Response surface optimization process via ANSYS DesignXplorer.

A: Model_B: pure bending
 Deformation of nine parts
 Type: total deformation
 Unit: mm
 Time: 1

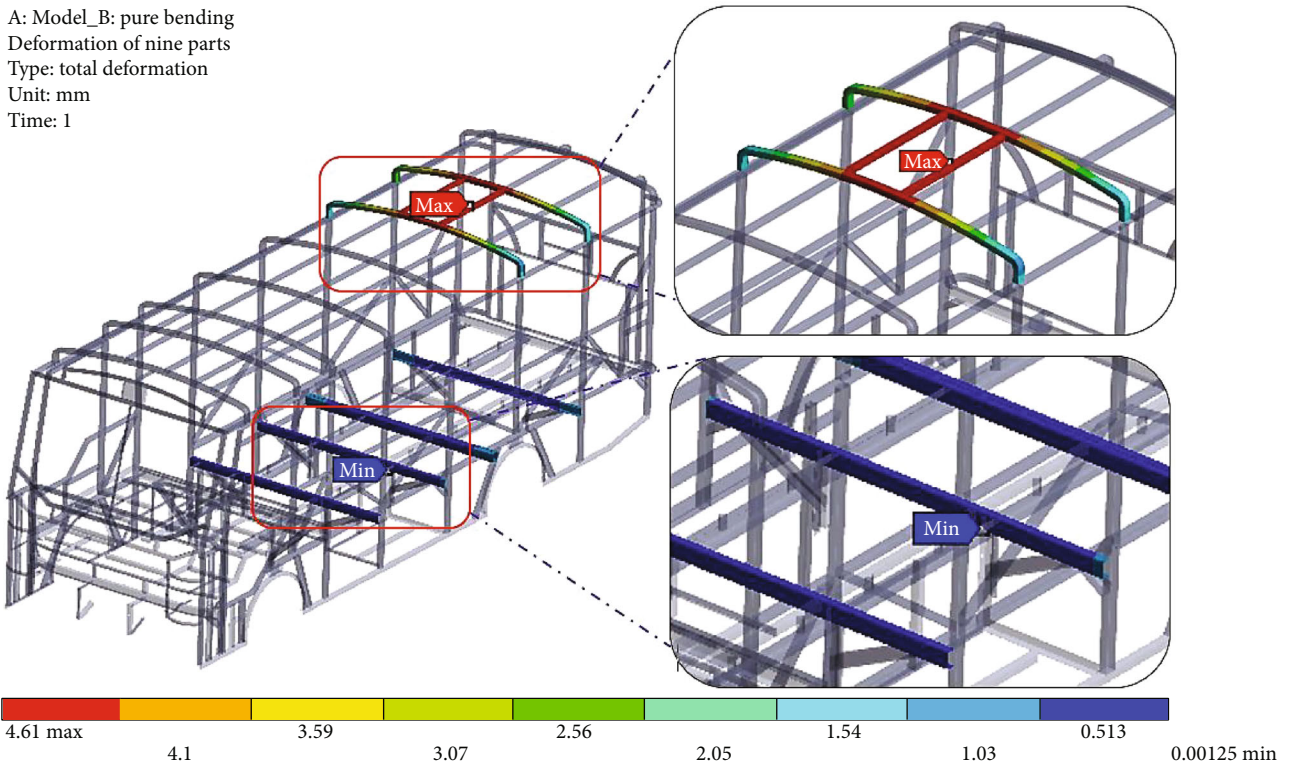


FIGURE 10: Preliminary FE results of the reinforced structure on the floor and roof sections.

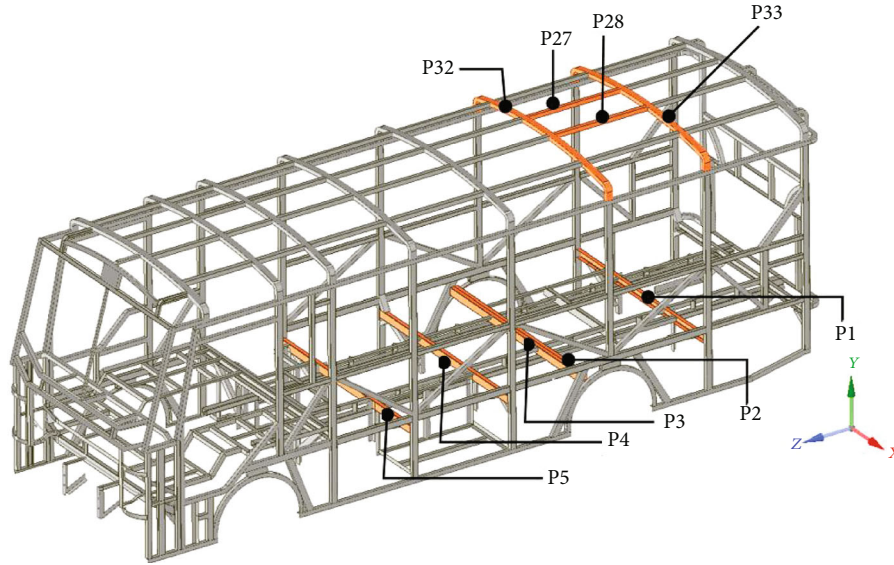


FIGURE 11: Selected parts of the reinforced structure.

TABLE 5: Cross section and levels of thickness of selected parts.

Sections	Selected parts	Cross section	Thickness (mm)	Ranges of mfg. values (mm)
Floor	P1–P5	C-channel	3	1, 1.5, 2, 2.5, 3
Roof	P27, P28, P32, and P33	SHS	1.5	1, 1.5, 2, 2.5, 3

Relative average absolute error (RAAE):

$$RAAE = \frac{1}{N\sigma_r} \sum_{j=1}^N |r_j - \tilde{r}_j|. \quad (7)$$

During goodness of fit, when determining the best quality of the fit for responses, the coefficient of determination (R^2) should be higher and equal to 1 [2]. Accordingly, the perfect fit ($R^2 = 1$) was found for all parts of the mass response, as seen in Table 6. Moreover, the R^2 of the total deformation response equals 0.995. Generally, the effect of fitting in all output responses is good. All errors measured by using the ANSYS statistical tool are tiny except the relative maximum absolute error (RMAE).

The response surface optimization (RSO) method serves as an objective function for the MOGA in ANSYS Workbench [5]. The multiobjective genetic algorithm (MOGA) uses a genetic algorithm to support many objectives and constraints at the comprehensive optimum finding [41]. Moreover, MOGA quickly optimized many design variables based on NSGA-II (Nondominated Sorting Genetic Algorithm II) [23]. The interactive approach considers the constraint approach with two functions (objective and constraint) to identify a single best compromise solution as a form of [35]

$$\begin{aligned} &\text{minimize} && f_1(t) \\ &\text{subject to} && f_2(t) \leq c \\ &\text{and} && t \in \Gamma, \end{aligned} \quad (8)$$

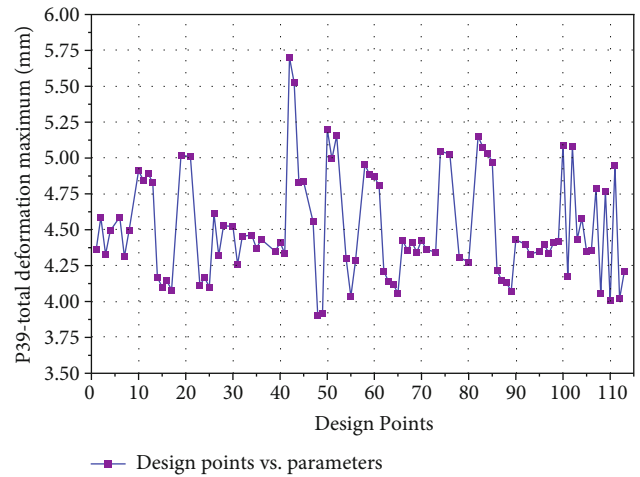


FIGURE 12: Total deformation (maximum) parameter at each design point.

where Γ is the sets of the lower and the upper bounds on input variable ($t_L \leq t \leq t_U$) and c is the bounds of the outputs ($c_{\min} \leq c \leq c_{\max}$).

The genetic algorithm (GA) is broadly used in structural optimization due to the advantage of simple operation and accurate optimal solution with fast convergence speed [20, 42, 43]. From design points and response surface curves, the several values of total deformation occurred below 4.25 mm. Compared to the reinforced model, reducing the total deformation below 4.25 mm is also possible. Thus, it is decided that the constraint of deformation is less than or equal to 4.25 mm. In this section, the design objective and

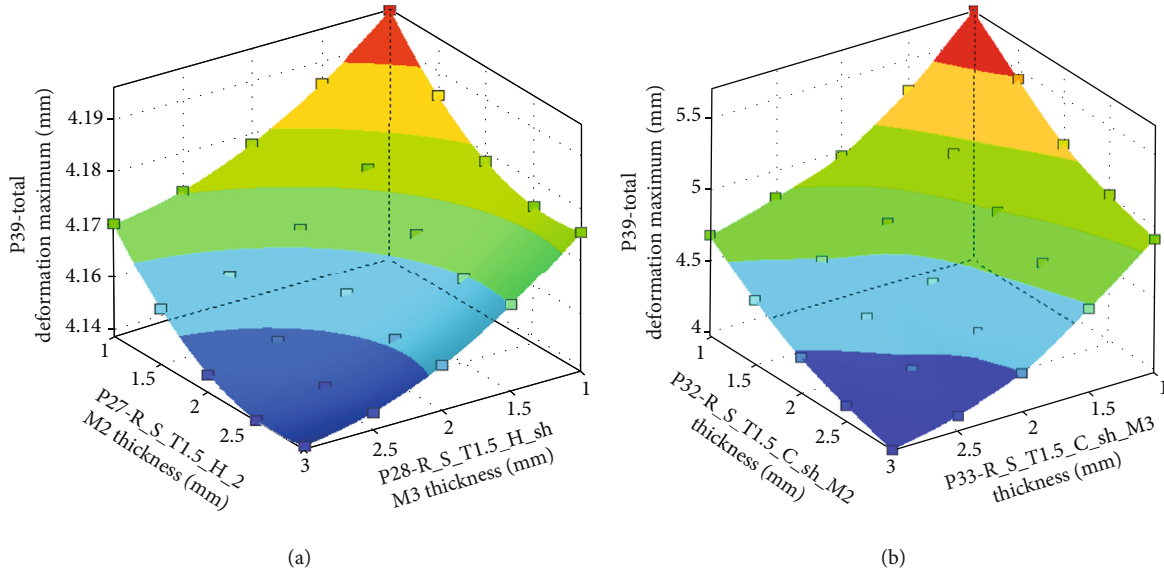


FIGURE 13: Representation of the 3D response surface for four input variables.

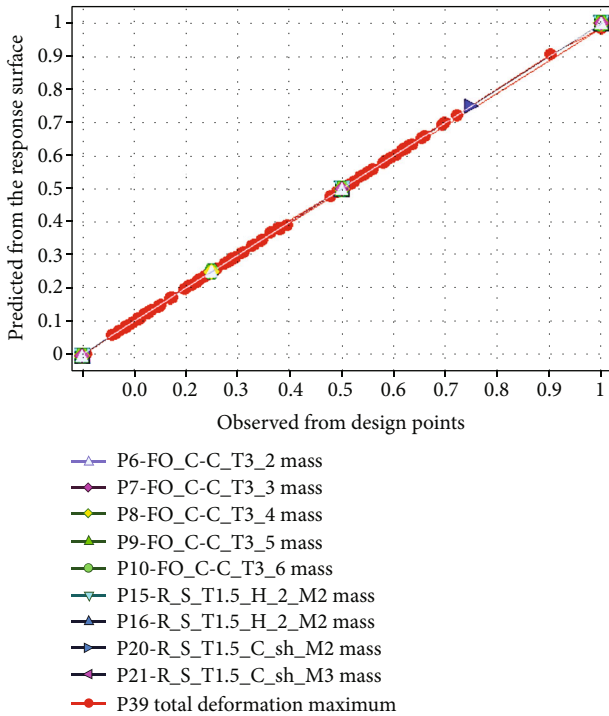


FIGURE 14: Illustration of the goodness of fit for the observed and predicted results.

constraints are set up using the multiobjective genetic algorithm (MOGA) in response surface optimization. These are as follows:

- (i) Minimize the mass of roof and floor parts
- (ii) Subject it to total deformation ≤ 4.25 mm

The optimization task initially produces 9,000 samples and assigns 1,800 samples (per iteration) and 20 iterations

to acquire three candidate points. The optimization also converged after 10,591 evaluations.

The most significant candidate design point is obtained by searching for the best objective function value over the vast feasible region of the design spaces [26, 44]. After optimization runs, the three (3) design candidates are determined, as shown in Table 7. Moreover, Table 7 also depicts the optimum output parameters (mass and deformation) of nine design variables by RSO with the MOGA method. Thus, the candidates give less deformation value with the reduced mass of the nine selected parts than the current (original) design value. However, the optimum design candidate was carefully chosen to simultaneously satisfy optimum deformation and mass reduction values. Afterwards, the thickness of the nine parts can be consistent for manufacturing. The value of maximum deformation of candidate 2 is higher than others. So, the selection of an optimum candidate design is considered between candidate points 1 and 3. However, candidate point 1 (CP-#1) is an optimal design candidate due to reduced mass and deformation with possible manufacturable thickness values, as shown in Table 7.

Figure 15 describes the sensitivities of the outputs with input thickness. These sensitivities imply that all thickness parts are positively correlated with direct impacts for mass outputs (instead of deformation). Moreover, only three thickness parameters (P1, P32, and P33) negatively correlate with the maximum total deformation. They also have some amounts of influence but inversely.

3. Result and Discussion

In the pure bending load mode, the original model of the bus structure has the most considerable deformation (6.2–6.5 mm) located at the location of the luggage on roof parts (see Figure 16(a)). The maximum deformation of the reinforced model was 4.6 mm, and the minimum deformation was located at the frontal parts, passenger compartment parts, and frontal-side part of the structure, as shown in Figure 16(b)).

TABLE 6: Accuracy of the goodness of fit in the response surface (RS).

ANSYS statistical metrics	Output parameters (mass and total deformation)									
	P6	P7	P8	P9	Masses			Deformation		
					P10	P15	P16	P20	P21	P39
R^2	1	1	1	1	1	1	1	1	1	0.995
RMSE	$2.2E-10$	$2.0E-10$	$1.9E-10$	$2.0E-10$	$1.8E-10$	$2.7E-10$	$1.7E-10$	$5.9E-10$	$9.8E-10$	0.025
RMAE	$4.1E-08$	$3.3E-08$	$3.2E-08$	$3.2E-08$	$2.9E-08$	$1.2E-07$	$8.8E-08$	$1.4E-07$	$1.3E-07$	48.85
RAAE	$1.1E-08$	$9.9E-09$	$8.2E-09$	$9.7E-09$	$8.3E-09$	$2.6E-08$	$1.2E-08$	$1.2E-08$	$2.9E-08$	3.27

R^2 : coefficient of determination. The bold value in all output responses (mass and deformation) shows the best fit value.

TABLE 7: Candidate points (CP) obtained from RSO.

	Thickness (mm)									Total mass of the parts (kg)	Max. deformation (mm)
	P1	P2	P3	P4	P5	P27	P28	P32	P33	P6-P10, P15, P16, P20, and P21	P39
Original value	3	3	3	3	3	1.5	1.5	1.5	1.5	53.42	4.61
CP-#1	2.5	1.5	1	1	1	1	1	2.5	2.5	39.08	4.19
CP-#2	1	3	1	1	1	1	1	2.5	3	40.94	4.23
CP-#3	2	1.5	1	1.5	1	1	1	2.5	3	40.94	4.11

The original value shows the thickness and mass of the selected parts and the maximum deformation of the structure before optimization.

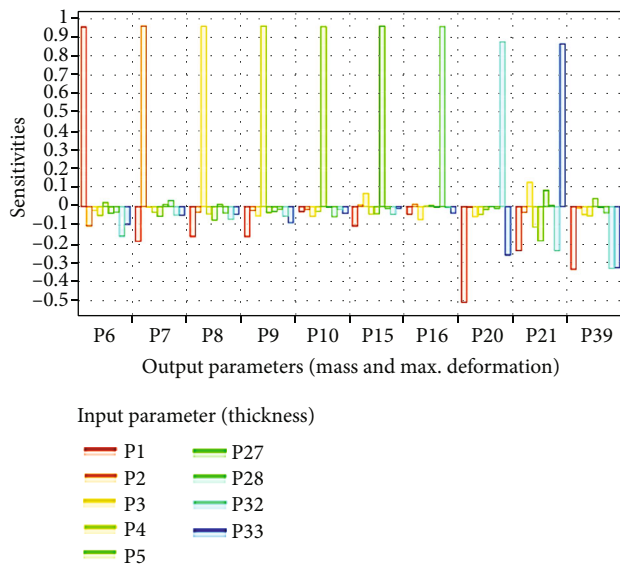


FIGURE 15: Sensitivities of output responses.

The total deformation of the reinforced model in pure bending decreased by 29.4%. In addition, RSO by the MOGA approach also reduced the deformation of the reinforced model by 9.11%. Accordingly, the reduction of deformation showed that the reinforced design is stiffer than the original design. Moreover, the optimized design has a lower deformation than the reinforced and original design.

In the pure bending loading case, the equivalent stress of bus structure is decreased from 232 MPa to 213.35 MPa by reinforcement design, as shown in Figure 17. Moreover, the equivalent stress of model II (RSO) is equal to 219 MPa. The maximum equivalent stress is placed at the floor supports (hole of bolted parts).

The most considerable deformation of the baseline (original) model is 6.32 mm, which is still located on the roof luggage of the bus structure, as seen in Figure 18. Furthermore, the maximum deformation of the reinforced model is 5.6 mm and occurs at the frontal structure. However, RSO using the MOGA method also reduced the deformation of the reinforced model by 3.57%.

The most considerable equivalent stresses of the baseline model, model I, and model II are 230 MPa, 221.62 MPa, and 229 MPa, respectively, as shown in Figure 19. The maximum equivalent stresses are located at floor parts and bolted parts (hole of the L-shaped frame) for all models. Moreover, the reinforced model has less equivalent stress in the torsional load case than the other models.

The output parameters such as maximum equivalent stress, torsional stiffness, and deformation of the bus structure under two loading conditions in the static strength analysis are displayed in Table 8. Moreover, the maximum equivalent stress of the structure should not exceed the material's yield stress and meet the strength conditions [45]. Accordingly, all maximum stresses of models were obtained below the yield strength of the material, as shown in Table 8. First of all, the weight of a bus structure reduced from 577.35 kg to 547.15 kg. This result indicates that removing the connecting member (U-channel) from the side section and adding the inclined supports can effectively reduce the structure's weight. Furthermore, the response surface optimization via the MOGA method minimized the reinforced model from 547.15 kg to 532.70 kg through the variation of thickness of the roof and floor parts of the structure.

The bending stiffness difference between the original and reinforced models is 41.65%. Moreover, the bending stiffness of the optimized (RSO) model increases by 10.02% compared to that of the reinforced model. In addition, a reinforced bus structure's torsional rigidity or stiffness

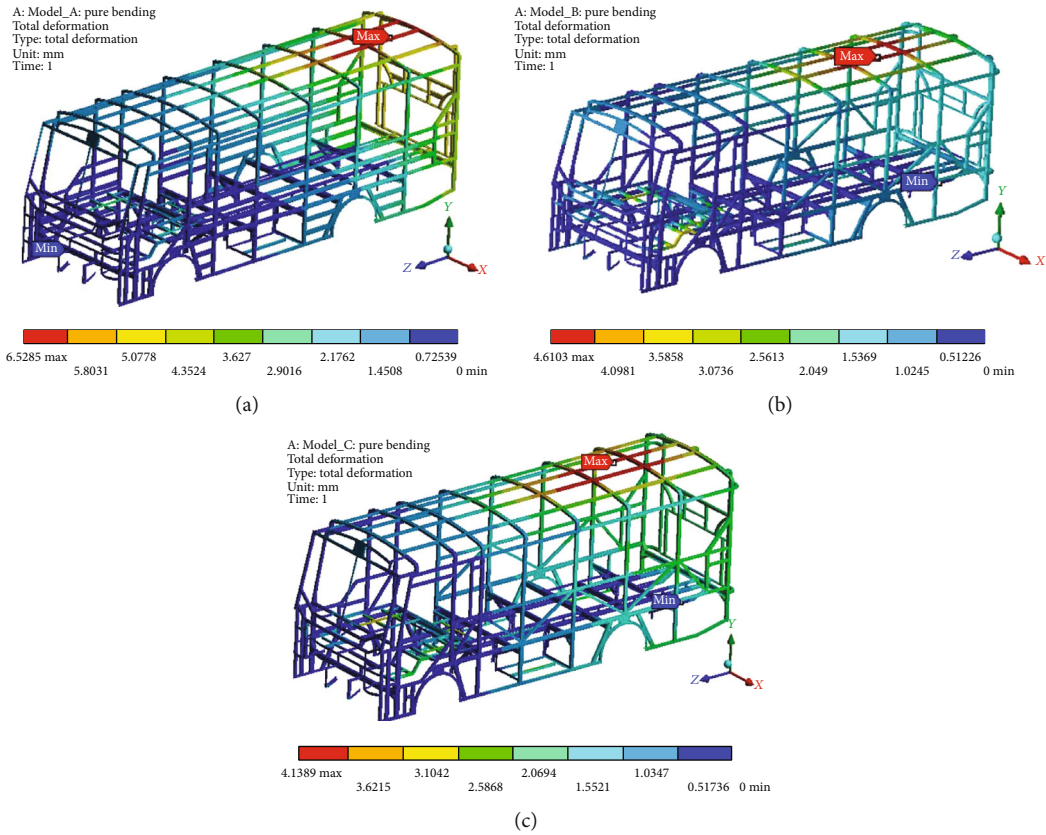


FIGURE 16: Total deformation in pure bending: (a) baseline model; (b) model I (RD); (c) model II (RSO).

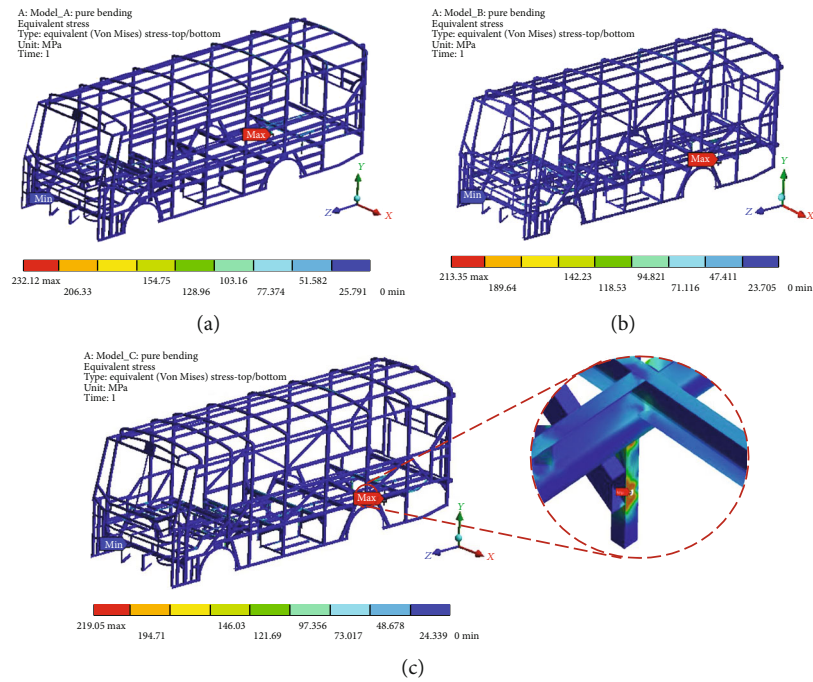


FIGURE 17: Equivalent stress in pure bending: (a) baseline model; (b) model I (RD); (c) model II (RSO).

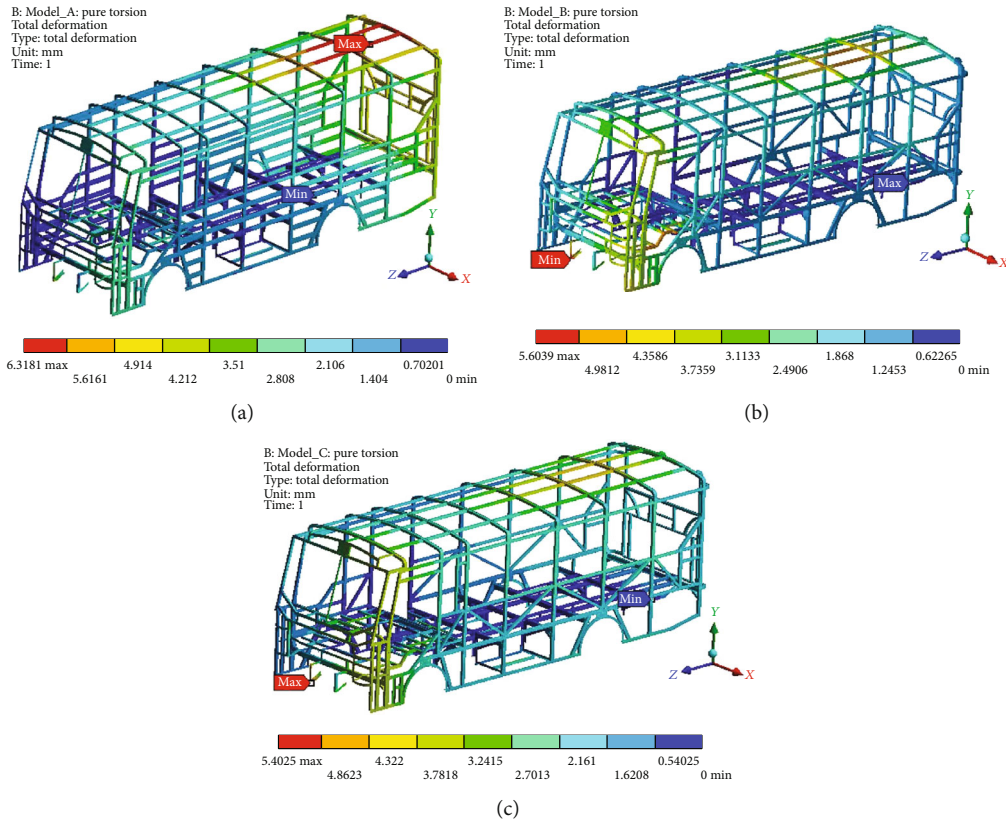


FIGURE 18: Total deformation in pure torsion: (a) baseline model; (b) model I (RD); (c) model II (RSO).

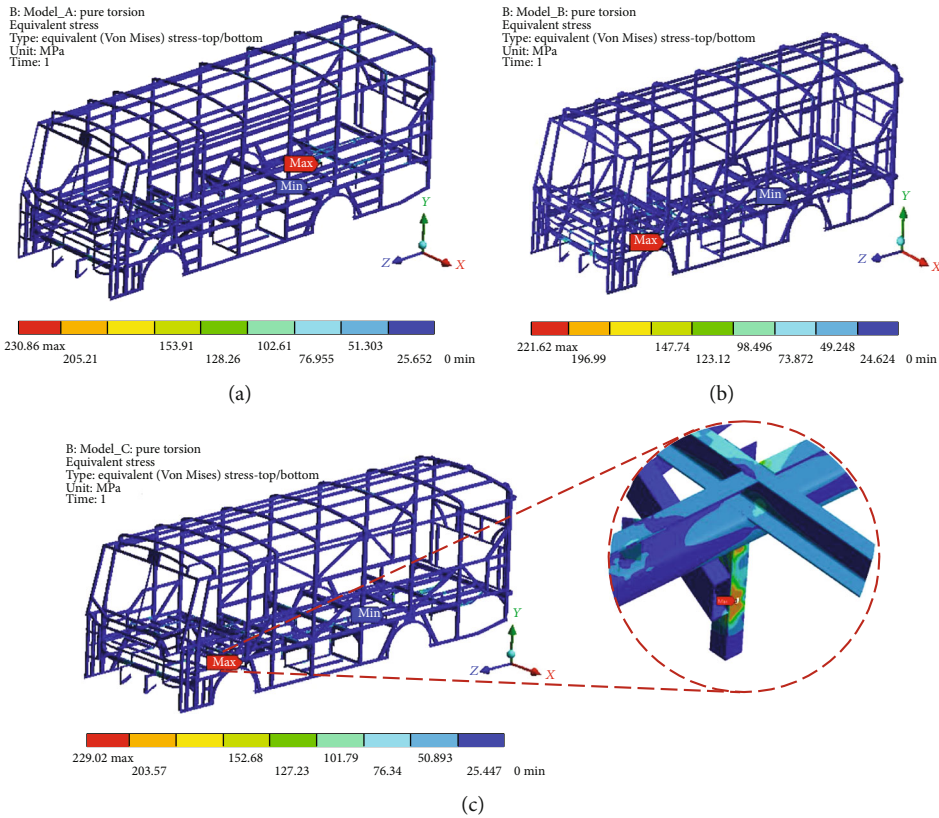


FIGURE 19: Equivalent stress in pure torsion: (a) baseline model; (b) model I (RD); (c) model II (RSO).

TABLE 8: Comparison of the original, reinforced, and optimal models in two loading conditions.

Loading conditions		Baseline design	Model I (RD)	Model II (RSO)
Pure bending	Total deformation (mm)	6.53	4.61	4.19
	Equivalent stress (MPa)	232.12	213.35	219.05
	Bending stiffness (N/mm)	4589.5	6500.9	7152.6
Pure torsion	Total deformation (mm)	6.32	5.60	5.40
	Equivalent stress (MPa)	230.86	221.62	229.02
	Torsional stiffness (Nm/deg)	1379.93	1553.24	1604.31
	Angle of rotation (deg)	0.84	0.74	0.69
Bus structure	Total mass (kg)	577.35	547.15	532.70

increases from 1379.93 Nm/deg to 1553.24 Nm/deg. However, the difference in torsional stiffness among the reinforced vs. optimized models is 51.07 Nm/deg. This result found that the reinforced design and response surface optimization with MOGA must be considered to obtain the stiffed structure during the static condition.

4. Conclusion

This research facilitates the static analysis of a midibus structure using numerical methods (ANSYS). Moreover, this research also develops the optimized design of the structure through reinforcement and response surface optimization (RSO) methods. Consequently, the obtained results of static strength analysis and optimization can be summarized as follows:

- (i) In the baseline model, the maximum deformations occurred at the roof luggage and the top of rear frames for all loading conditions except the pure torsion case. Furthermore, the maximum equivalent stresses are located at floor parts and bolted support parts (hole of the L-shaped frame) of the original structure for all loading conditions
- (ii) From suggested approaches, firstly, the high stiffness within the reduced weight of the reinforced design is obtained by changing the layout, cross section, and reinforcement of the baseline structure. Secondly, the best-optimized design is also determined by response surface optimization (RSO) of the reinforced structure by changing the thickness of the roof and floor parts of the reinforced design

Overall, it can be concluded that the reinforcement design and response surface optimization can increase the stiffness and minimize the structure's weight for all loading conditions. However, perhaps the response surface optimization with the MOGA approach gives better strength with a lightweight structure.

Data Availability

The data required to produce these findings cannot be shared as the data also form part of an ongoing study at this time.

Conflicts of Interest

The authors state that there are no conflicts of interest.

Acknowledgments

The authors highly acknowledge the local bodybuilders located in Ethiopia, the Federal and Oromia Minister of Transport, and Addis Ababa University for the essential continuous support of their resources and vital information for this research.

References

- [1] Z. Luo, X. Zhao, L. Liang, and F. Wang, "Structural optimization of slender robot arm based on sensitivity analysis," *Mathematical Problems in Engineering*, vol. 2012, 2012.
- [2] J. Zhang, W. Ran, and X. Qi, "Optimal design of an electric vehicle frame based on response surface analysis," *Converter Magazine*, vol. 2021, no. 7, pp. 151–165, 2021.
- [3] D. Crococolo, M. De Agostinis, and N. Vincenzi, "Structural analysis of an articulated urban bus chassis via FEM: a methodology applied to a case study," *Strojniški vestnik-Journal of Mechanical Engineering*, vol. 57, no. 11, pp. 799–809, 2011.
- [4] S. Rooppakhun and J. Wichairahad, "The strength analysis of a bus superstructure based on the accuracy improvement of T-junction flexible joint stiffness," *International Journal of Engineering & Technology*, vol. 7, no. 3, pp. 62–67, 2018.
- [5] C. Reyes-ruiz, O. R. Cervantes, A. O. Prado, and E. Ramirez, "Analysis and optimization of a passenger bus frame through finite element software," in *2013 SIMULIA Community Conf.*, 2013.
- [6] H. Wang, X. Jin, and Z. Lin, "FEM static and dynamic analysis of the body structure of SK6120 low floor city bus," *SAE Technical Paper*, 2002.
- [7] F. Lan, J. Chen, and J. Lin, "Comparative analysis for bus side structures and lightweight optimization," *Proceedings of the Institution of Mechanical Engineers, Part D: Journal of Automobile Engineering*, vol. 218, no. 10, pp. 1067–1075, 2004.
- [8] Z. Yang, B. Deng, M. Deng, and G. Sun, "A study on finite element analysis of electric bus frame for lightweight design," in *MATEC Web of Conferences*, vol. 175, pp. 1–4, 2018.
- [9] X.-C. WU, W.-Q. ZHENG, and P. ZHOU, "Topology optimization design of bus body structure based on Altair-optiS-struct," in *Proceedings of the 2014 International Conference on Mechanics and Civil Engineering*, vol. 7no. Icmce, pp. 281–286, 2014.

- [10] T. Pravilonis, E. Sokolovskij, A. Kilikevičius, J. Matijošius, and K. Kilikevičienė, "The usage of alternative materials to optimize bus frame structure," *Symmetry*, vol. 12, no. 6, 2020.
- [11] A. Y. Ismail, G. Na, and B. Koo, "Topology and response surface optimization of a bicycle crank arm with multiple load cases," *Applied Sciences*, vol. 10, no. 6, 2020.
- [12] M. J. L. B., B. L. B. A. Gauchia and V. Diaz, "Torsional stiffness and weight optimization of a real bus structure," *International Journal of Automotive Technology*, vol. 11, no. 1, pp. 41–47, 2010.
- [13] W. Zhong, R. Su, L. Gui, and Z. Fan, "Multi-objective topology and sizing optimization of bus body frame," *Structural and Multidisciplinary Optimization*, vol. 54, no. 3, pp. 701–714, 2016.
- [14] T. Kim, "Study on the stiffness improvement of bus structure," Tech. Rep. 412, SAE Technical Papers, 1993.
- [15] Y. Feng, C. Wang, B. Briseghella, L. Fenu, and T. Zordan, "Structural optimization of a steel arch bridge with genetic algorithm," *Structural Engineering International*, vol. 31, no. 3, pp. 347–356, 2021.
- [16] H.-S. Kang, I.-J. Hwang, and Y.-J. Kim, "Optimal design of impeller shroud for centrifugal compressor using response surface method," *The KSFM Journal of Fluid Machinery*, vol. 18, no. 4, pp. 43–48, 2015.
- [17] A. Muhammad, I. Shanono, and I. H. Shanono, "Static Analysis and Optimization of a Connecting Rod," *Artic. Int. J. Eng. Technol. Sci.*, vol. 6, pp. 24–40, 2019.
- [18] C. Mi, Z. Huang, L. I. Wentai et al., "Multi-objectives optimization design of a-type frame in an electric mining dump truck considering multi-source uncertainties based on the interval method," *Mechanics*, vol. 27, no. 2, pp. 168–174, 2021.
- [19] A. Hadadian, R. Sedaghati, and E. Esmailzadeh, "Design optimization of magnetorheological fluid valves using response surface method," *Journal of Intelligent Material Systems and Structures*, vol. 25, no. 11, pp. 1352–1371, 2014.
- [20] B. L. Boada, A. Gauchia, M. J. L. Boada, and V. Diaz, "A genetic-based optimization of a bus structure as a design methodology," in *12th IFToMM World Congress*, pp. 18–21, Besancon, 2007.
- [21] P. K. Choudhary, P. K. Mahato, and P. Jana, "Optimization of surface-profile of orthotropic cylindrical shell for maximizing its ultimate strength," *Mechanics of Advanced Materials and Structures*, pp. 1–13, 2021.
- [22] Y. Zhang, L. He, J. Yang, G. Zhu, X. Jia, and W. Yan, "Multi-objective optimization design of a novel integral squeeze film bearing damper," *Machines*, vol. 9, no. 10, 2021.
- [23] B. Zheng, X. Wang, and J. Zhang, "Structure optimization design for brake drum based on response surface methodology," *Manufacturing Technology*, vol. 21, no. 3, pp. 413–420, 2021.
- [24] W.-X. Ren, S.-E. Fang, and M.-Y. Deng, "Response surface-based finite-element-model updating using structural static responses," *Journal of Engineering Mechanics*, vol. 137, no. 4, pp. 248–257, 2011.
- [25] S. Wu, J. Xing, L. Dong, and H. Zhu, "Multi-objective optimization of microstructure of gravure cell based on response surface method," *PRO*, vol. 9, no. 2, pp. 1–15, 2021.
- [26] X. Chen and Y. Liu, *Finite Element Modeling and Simulation with ANSYS Workbench*, CRC press, 2018.
- [27] ANSYS Help System, *ANSYS Mechanical User's Guide*, vol. 3304, Release 15, ANSYS, Inc., 2012.
- [28] P. Kandekar, B. Patil, K. Kulkarni et al., "Design and development of alternative method for vibration issues in locomotive wagon wheels," in *Journal of Physics: Conference Series*, vol. 1706no. 1IOP Publishing.
- [29] I. Kernyskyy, Y. Yakovenko, O. Horbay et al., "Development of comfort and safety performance of passenger seats in large city buses," *Energies*, vol. 14, no. 22, p. 7471, 2021.
- [30] A. Hari Kishan and P. Kondalarao, "Transient structural analysis of electric bus chassis frame," in *IOP Conf. Ser. Materials Science and Engineering*, vol. 1185, 2021no. 1.
- [31] T. Pravilonis, V. Eidukynas, and E. Sokolovskij, "An analysis of the reliability of a bus safety structure on carrying out the numerical and experimental tests," *Sensors*, vol. 20, no. 24, pp. 1–15, 2020.
- [32] J. Zhang and W. Ran, "Lightweight optimization design of a light electric commercial vehicle frame," *Journal of Physics Conference Series*, vol. 1, p. 2021, 1939.
- [33] J. Na, Z. Yuan, and J. Gao, "A novel method for bending stiffness evaluation of bus body," *Advances in Mechanical Engineering*, vol. 7, no. 1, 2015.
- [34] A. Gauchia, B. L. Boada, M. J. L. Boada, and V. Diaz, "Integration of MATLAB and ANSYS for advanced analysis of vehicle structures," *MATLAB applications for the practical engineer*, vol. 2017, 2014.
- [35] A. D. Belegundu and T. R. Chandrupatla, *Optimization Concepts and Applications in Engineering*, Cambridge University Press, 3rd edition, 2019.
- [36] C. Bojanowski, *Verification, Validation and Optimization of Finite Element Model of Bus Structure for Rollover Test*, Florida State University, 2009.
- [37] G. N. Vanderplaats, "Structural optimization for statics, dynamics and beyond," *Journal of the Brazilian Society of Mechanical Sciences and Engineering*, vol. 28, no. 3, pp. 316–322, 2006.
- [38] G. Liu, L. Guo, X. Wang, and Q. Wu, "Topology and parametric optimization based lightweight design of a space reflective mirror," *Optical Engineering*, vol. 57, no. 7, p. 1, 2018.
- [39] K. Alawadhi, B. Alzuwayer, T. A. Mohammad, and M. H. Buhemdi, "Design and optimization of a centrifugal pump for slurry transport using the response surface method," *Machines*, vol. 9, no. 3, 2021.
- [40] S. Abbasi and A. Gholamalipour, "Performance optimization of an axial turbine with a casing injection based on response surface methodology," *Journal of the Brazilian Society of Mechanical Sciences and Engineering*, vol. 43, no. 9, pp. 1–15, 2021.
- [41] ANSYS 2020 R1, *ANSYS DesignXplorer User's Guide*, vol. 15317, ANSYS, Inc., 2021.
- [42] G. Lai, J. Liu, and F. Zeng, "Application of multi-objective genetic algorithm in ship shafting alignment optimization," in *Proceedings -2017 10th International Symposium on Computational Intelligence and Design, ISCID 2017*, vol. 2, pp. 275–278, 2018.
- [43] W. Feng and W. H. Yong, "Optimization design of a bus body frame," in *Advanced Materials Research*, vol. 605, pp. 600–603, Trans Tech Publications Ltd, 2013.
- [44] G. Grebenişan and N. Salem, "The multi-objective genetic algorithm optimization, of a superplastic forming process, using ansys®," in *MATEC Web of Conferences*, vol. 126, 2017.
- [45] Y. H. Wang, C. Zhang, Y. Q. Su, L. Y. Shang, and T. Zhang, "Structure optimization of the frame based on response surface method," *International Journal of Structural Integrity*, vol. 11, no. 3, pp. 411–425, 2020.